International Journal of Minerals, Metallurgy and Materials
Volume 23, Number 3, March 2016, Page 283
DOI: 10.1007/s12613-016-1237-9

Coarsening behavior of MX carbonitrides in type 347H heat-resistant austenitic steel during thermal aging

Ying-hui Zhou, Chen-xi Liu, Yong-chang Liu, Qian-ying Guo, and Hui-jun Li

State Key Lab of Hydraulic Engineering Simulation and Safety, School of Materials Science and Engineering, Tianjin University, Tianjin 300072, China
(Received: 3 July 2015; revised: 12 September 2015; accepted: 14 September 2015)

Abstract: In this work, the growth kinetics of MX (M = metal, X = C/N) nanoprecipitates in type 347H austenitic steel was systematically studied. To investigate the coarsening behavior and the growth mechanism of MX carbonitrides during long-term aging, experiments were performed at 700, 800, 850, and 900°C for different periods (1, 24, 70, and 100 h). The precipitation behavior of carbonitrides in specimens subjected to various aging conditions was explored using carbon replicas and transmission electron microscopy (TEM) observations. The corresponding sizes of MX carbonitrides were measured. The results demonstrates that MX carbonitrides precipitate in type 347H austenitic steel as Nb(C,N). The coarsening rate constant is time-independent; however, an increase in aging temperature results in an increase in coarsening rate of Nb(C,N). The coarsening process was analyzed according to the calculated diffusion activation energy of Nb(C,N). When the aging temperature was 800–900°C, the mean activation energy was 294 $kJ \cdot mol^{-1}$, and the coarsening behavior was controlled primarily by the diffusion of Nb atoms.

Keywords: austenitic steel; heat resistance; carbonitrides; coarsening; nanoparticles; diffusion; thermal aging

1. Introduction

Austenitic heat-resistant steel is widely used in applications involving temperatures greater than 600°C because of its excellent corrosion resistance and mechanical properties at high temperatures. Type 347H austenitic steel, as one of the series of 18Cr–8Ni austenite stainless steels, is commonly used in thermal power plants and other industries. The important role of precipitation in achieving good creep properties of heat-resistant steels has long been recognized. One of the most effective ways to improve the creep properties is to attain fine precipitates with long-term stability at elevated temperatures [1–3].

$M_{23}C_6$ carbides and MX carbonitrides (i.e., M = metal and X = C/N) are two primary precipitates in type 347H austenitic steel. MX carbonitrides effectively strengthen boundaries because they can act as obstacles to migrating boundaries [4]. In addition, compared to Laves phase and $M_{23}C_6$ carbides in type 347H austenitic steel, the MX carbonitrides exhibit the smallest size. The stability of MX nanoprecipitates is critical to retaining the high-temperature strength and creep resistance of austenitic heat-resistant steels [5].

Considerable work exploring the coarsening behavior of carbonitrides in steels has been reported [6–9]. Research on austenitic stainless steels has focused on the size, microstructure, and precipitation sites of carbonitrides, whereas little attention has been devoted to the coarsening mechanism of MX carbonitrides. For example, Gustafson and Hättestrand [10] investigated the coarsening of $M_{23}C_6$ precipitates in an Fe–Cr–C ternary alloy. Later, Gustafson [11] analyzed the carbides in 9% chromium steel using quantitative microscopy and simulations and observed that the V/Nb ratio had almost no effect on the coarsening rate, whereas N exhibited a strong effect. Hong *et al.* [3] observed that $M_{23}C_6$ precipitates in a strained sample formed significantly earlier than those in an unstrained specimen. Tan *et al.* [7] explored the stability of MX-type strengthening nanoprecipitates in ferritic steels under thermal aging, stress, and ion irradiation. Because the sizes of MX carbonitrides are so small, previous investigations have been focused primarily on the coarsening behavior of $M_{23}C_6$ carbides. MX carboni-

Corresponding author: Yong-chang Liu E-mail: licmtju@163.com

trides are clearly desirable for achieving and maintaining good high-temperature performance of type 347H austenitic steel. Therefore, exploring the coarsening behavior of MX carbonitrides is also important.

In this paper, MX carbonitrides were investigated in terms of the coarsening behavior and microstructure evolution of type 347H austenitic steel. The microstructure of the steel under various aging conditions was analyzed using the carbon replica method. Furthermore, the size of the MX carbonitride precipitates was measured, and the corresponding diffusion activation energy and coarsening rate were calculated to clarify the coarsening mechanism of MX carbonitrides.

2. Experimental

The chemical composition of the type 347H austenitic steel used in the experiments is listed in Table 1. The specimens with a size of 10 mm × 10 mm × 10 mm were austenitized at 1150°C for 30 min and then cooled in water. To eliminate the initial residual stress formed during the rolling process, long-term aging experiments were conducted at 700, 800, 850, and 900°C for 1, 24, 70, and 100 h at each temperature. A schematic of the adopted heat treatment process is given in Fig. 1.

Table 1. Chemical composition of the investigated type 347H austenitic steel wt%

C	Cr	Ni	Nb	N	Mn	P	Mo	S	Fe
0.059	17.60	10.71	0.54	0.013	1.59	0.024	0.116	0.0008	Bal.

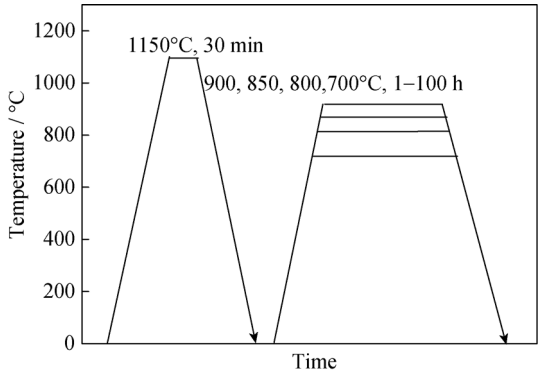

Fig. 1. Schematic of the heat treatment process of type 347H austenitic steel.

The thus-obtained specimens were etched with a mixed solution of $CuCl_2$:HCl:CH_3CH_2OH (1:20:20, by volume). The microstructures of the specimens were examined and their phases were identified by X-ray diffraction, scanning electron microscopy (SEM) in combination with energy-dispersive X-ray spectroscopy (EDS), and transmission electron microscopy (TEM) operated at a voltage of 200 kV.

The phase identification by X-ray diffraction was performed using an extraction method. The samples under various aging conditions were cut into slice-like specimens with dimensions of 10 mm × 10 mm × 2 mm. After being etched in a solution of hydrochloric acid for several days, the specimens were extracted using a centrifuge.

The precipitation behavior of carbonitrides in the type 347H austenitic steel specimens subjected to various aging treatments was investigated using the carbon replica method. The specimens were slid into a corrosive solution, and the replicas were collected by copper nets and dried. This method is highly efficient for observing the microstructure of MX carbonitrides. There were 800–1000 particles measured for specimens aged under each set of aging conditions.

3. Results and discussion

In this work, type 347H austenitic steel was heat treated at 700, 800, 850, and 900°C for various periods. Many granules with a size of approximately 50 nm were observed in the austenite matrix of isothermally treated samples (see Fig. 2(a)). According to the results shown in Figs. 2(b)–2(f), block-shaped particles in type 347H austenitic steel are Nb(C,N). In addition, some line-like or rod-like particles were distributed in the matrix. Figs. 2(g)–2(h) illustrate that these particles are Nb-rich MX carbonitrides. More importantly, Fig. 2(f) shows the XRD patterns of the specimen aged at 700°C for 100 h. As shown in the figure, all of the precipitates observed under high magnification (10000×) are Nb(C,N) carbonitrides; i.e., all of the particles measured using the nano-measurer software are Nb(C,N). Thus, the MX carbonitrides in the microstructure of the type 347H austenitic steel exhibit two different morphologies: rod-like and block-like particles.

3.1. Coarsening behavior of MX carbonitrides

3.1.1. TEM observations

Fig. 3 shows the TEM images of the type 347H austenitic steel specimens aged at 700°C for various periods. In the specimen aged at 700°C for 1 h (Fig. 3(b)), fine, square-shaped Nb(C,N) carbonitrides were distributed along and within the dislocation lines. We also observed some particles distributed in a dislocation line, which is consistent with the hypothesis that nucleation at dislocations effectively hinders the motion of dislocations and maintains the mechanical properties of steels at elevated temperatures [12–13]. When the aging time was increased to 100 h (Figs.

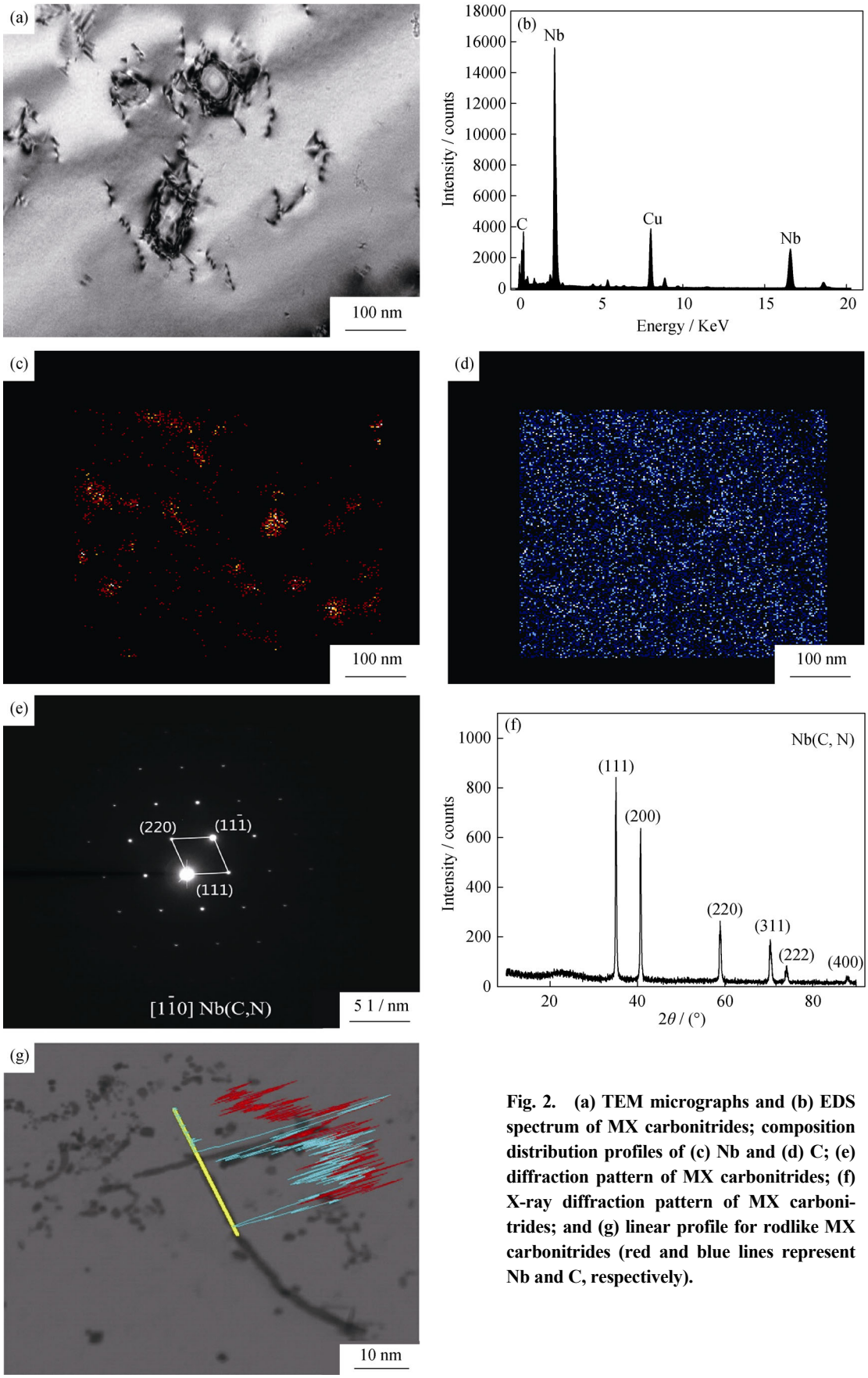

Fig. 2. (a) TEM micrographs and (b) EDS spectrum of MX carbonitrides; composition distribution profiles of (c) Nb and (d) C; (e) diffraction pattern of MX carbonitrides; (f) X-ray diffraction pattern of MX carbonitrides; and (g) linear profile for rodlike MX carbonitrides (red and blue lines represent Nb and C, respectively).

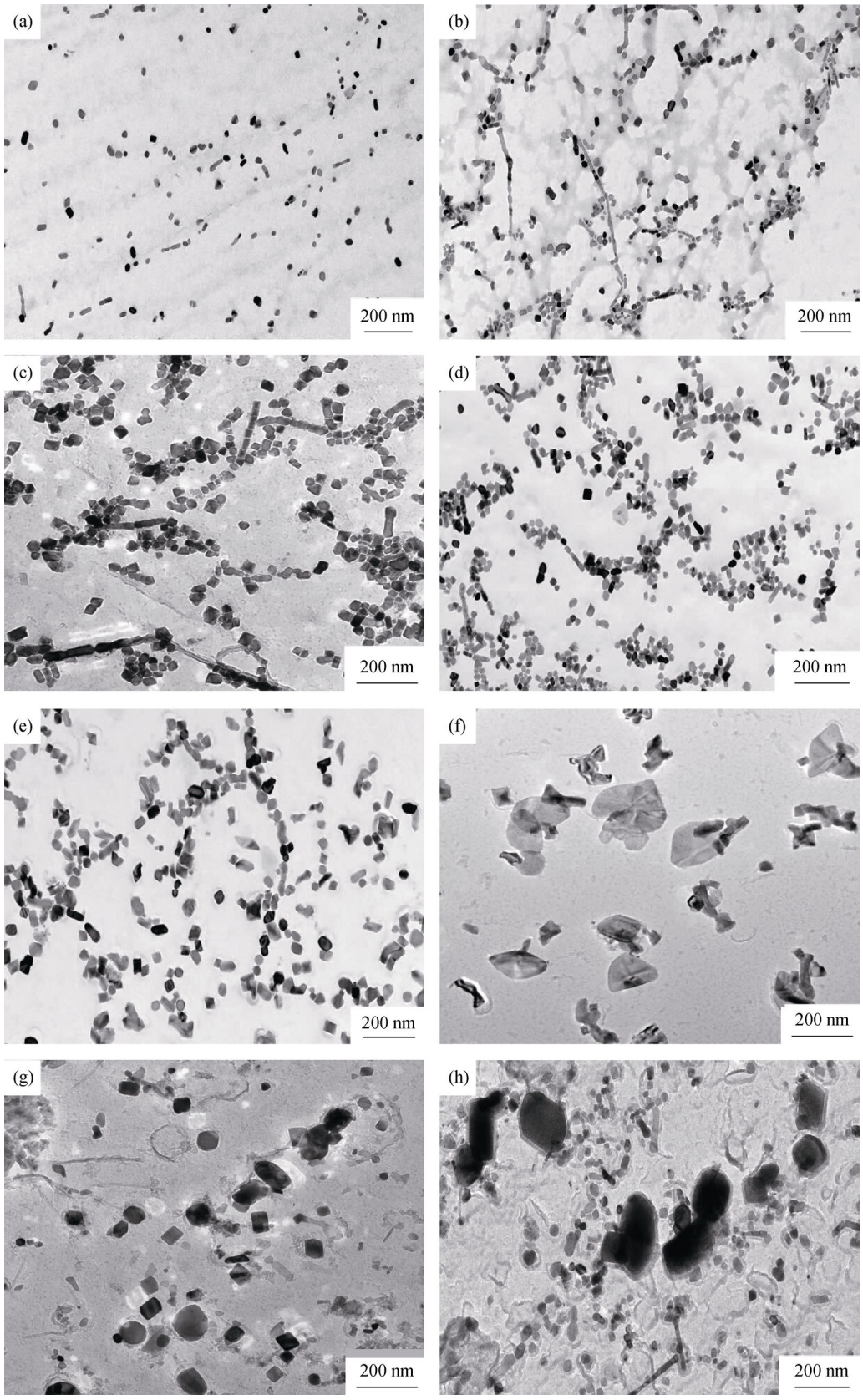

Fig. 3. Typical TEM micrographs of extraction replicas in type 347H steel aged at 700°C for different periods: (a) 0 h, (b) 1 h, (c) 24 h, (d) 70 h, (e) 100 h, (f) 500 h, (g) 1000 h, and (h) 2200 h.

3(b)–3(e)), the coarsening tendency of the original Nb(C,N) carbonitrides in the microstructure of the type 347H austenitic steel specimens was inconspicuous. After aging for 500 h, the specimens contained numerous carbonitrides that had grown to approximately 200 nm. The size of the Nb(C,N) precipitates increased with increasing aging time. In addition, at aging times of 500 h or longer (Fig. 3(f)), additional Nb(C,N) precipitated in the austenite matrix. Many of the fine freshly formed carbonitrides are located at dislocations and beneficially affect the high-temperature properties of the steel. Because of the coarsening of Nb(C,N) carbonitrides, the dislocation movement and the growth of grains cannot be effectively retarded, which is detrimental to the properties of type 347H austenitic steel. However, the precipitation of secondary Nb(C,N) particles may substantially contribute to precipitation strengthening.

Many nanosized Nb(C,N) particles were precipitated in the specimens isothermally aged at 700°C. To investigate the coarsening behavior of Nb(C,N) in austenitic steel at higher temperatures, we heat treated samples at 800, 850, and 900°C for 1, 24, 70, and 100 h, respectively. Fig. 4 shows TEM micrographs of Nb(C,N) precipitates in various type 347H austenitic steel specimens aged at 800, 850, and 900°C for different periods. The size of the Nb(C,N) precipitates clearly increased with increasing isothermal holding temperature. Moreover, in the case of the type 347H austenitic steel specimen aged at 700°C, secondary Nb(C,N) precipitated after 500 h, as illustrated in Figs. 3(a)–3(h). In contrast, in the case of the specimen aged at 800°C, secondary particles formed after 24 h (see Fig. 4(d)). These results suggest that an increase in the isothermal holding temperature facilitates the formation of secondary Nb(C,N) precipitates.

3.1.2. Quantitative analysis

Because a high-energy state of interfacial energy exists when numerous precipitates are distributed within an austenitic matrix, the phase interfaces exhibit an inevitable tendency to reduce the interfacial energy. The coarsening behavior of Nb(C,N) carbonitrides clearly follows the Ostwald ripening mechanism, i.e., the solute concentration around small-sized particles is greater than that around large-sized particles. Solute atoms will diffuse from surrounding small-sized particles into large-sized particles. This diffusion will not only disrupt the equilibrium state of solute concentration around the particles but also result in the dissolution of small particles and growth of large particles [14].

Quantification of the size distributions of the Nb(C,N) particles was conducted with various specimens of type 347H austenitic steel. Fig. 5 presents the size distribution histogram of Nb(C,N) particles in the steel specimens, and the average size of particles in the samples aged for different periods at 700°C is presented in Table 2. Notably, the mean size of the initial Nb(C,N) precipitates is 18.7 nm. As evident from the statistical data for all specimens aged at 700°C, the size of Nb(C,N) varies in the range from 20 to 100 nm when the annealing time is less than 500 h. When aged for 500 h, the Nb(C,N) precipitates become larger, in the size range from 100 to 200 nm. Although the size of the Nb(C,N) precipitates increases with increasing duration of the annealing periods, the main part of the Nb(C,N) precipitates still falls within the 20–100 nm range during aging at 700°C because an increasing number of secondary fine Nb(C,N) carbonitrides precipitates within the austenitic matrix; these precipitates are responsible for high-temperature strengthening effects observed in such steels. The present experimental observations also support this strengthening effect.

Similar size measurements of the Nb(C,N) carbonitrides were also performed for the type 347H austenitic steel specimens aged at 800, 850, and 900°C for different periods. Table 3 summarizes the average measured diameter of Nb(C,N) carbonitrides, and Fig. 6 illustrates the corresponding size distribution of Nb(C,N) carbonitrides in the type 347H austenitic steel samples aged at 800, 850, and 900°C for 24–100 h. In the case of specimens aged at 700°C, the size of the Nb(C,N) precipitates varies in the range from 20 to 40 nm, and the mean size is approximately 33.5 nm. In the case of the specimens aged at 900°C, more Nb(C,N) particles with sizes greater than 100 nm precipitate, and the mean size is approximately 56.4 nm. Although the measured average size of Nb(C,N) precipitates in the specimens aged at 900°C does not substantially differ from that of the precipitates in the specimens aged at 700°C, the kinetic coarsening process varies substantially among specimens isothermally annealed at temperatures ranging from 800°C to 900°C.

Here, the mean size of the Nb(C,N) precipitates was directly compared for the steel specimens annealed at temperatures ranging from 800°C to 900°C (see Table 3). Compared with the mean size of the Nb(C,N) precipitates in the steel specimen not subjected to an aging treatment, the size of the Nb(C,N) precipitates in the steel specimens aged for 100 h at 800, 850, and 900°C was 2.8, 5.2, and 9.4 times larger, respectively. That is, the coarsening behavior of Nb(C,N) carbonitrides is distinct, and the coarsening rate is accelerated when the isothermal treatment temperature is increased.

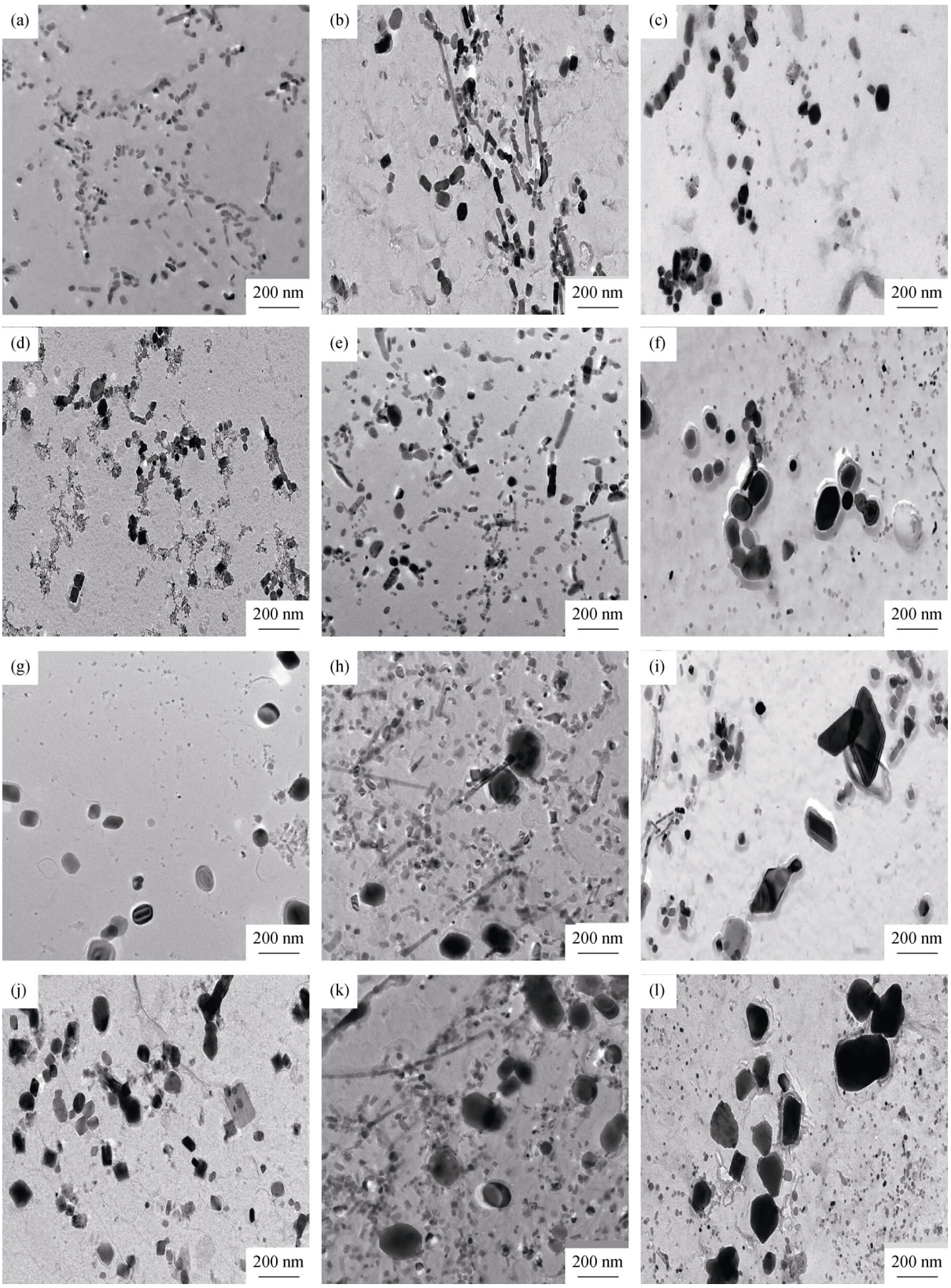

Fig. 4. Typical TEM micrographs of extraction replicas in type 347H steel aged at (a) 800°C for 1 h, (b) 850°C for 1 h, (c) 900°C for 1 h, (d) 800°C for 24 h, (e) 850°C for 24 h, (f) 900°C for 24 h, (g) 800°C for 70 h, (h) 850°C for 70 h, (i) 900°C for 70 h, (j) 800°C for 100 h, (k) 850°C for 100 h, and (l) 900°C for 100 h.

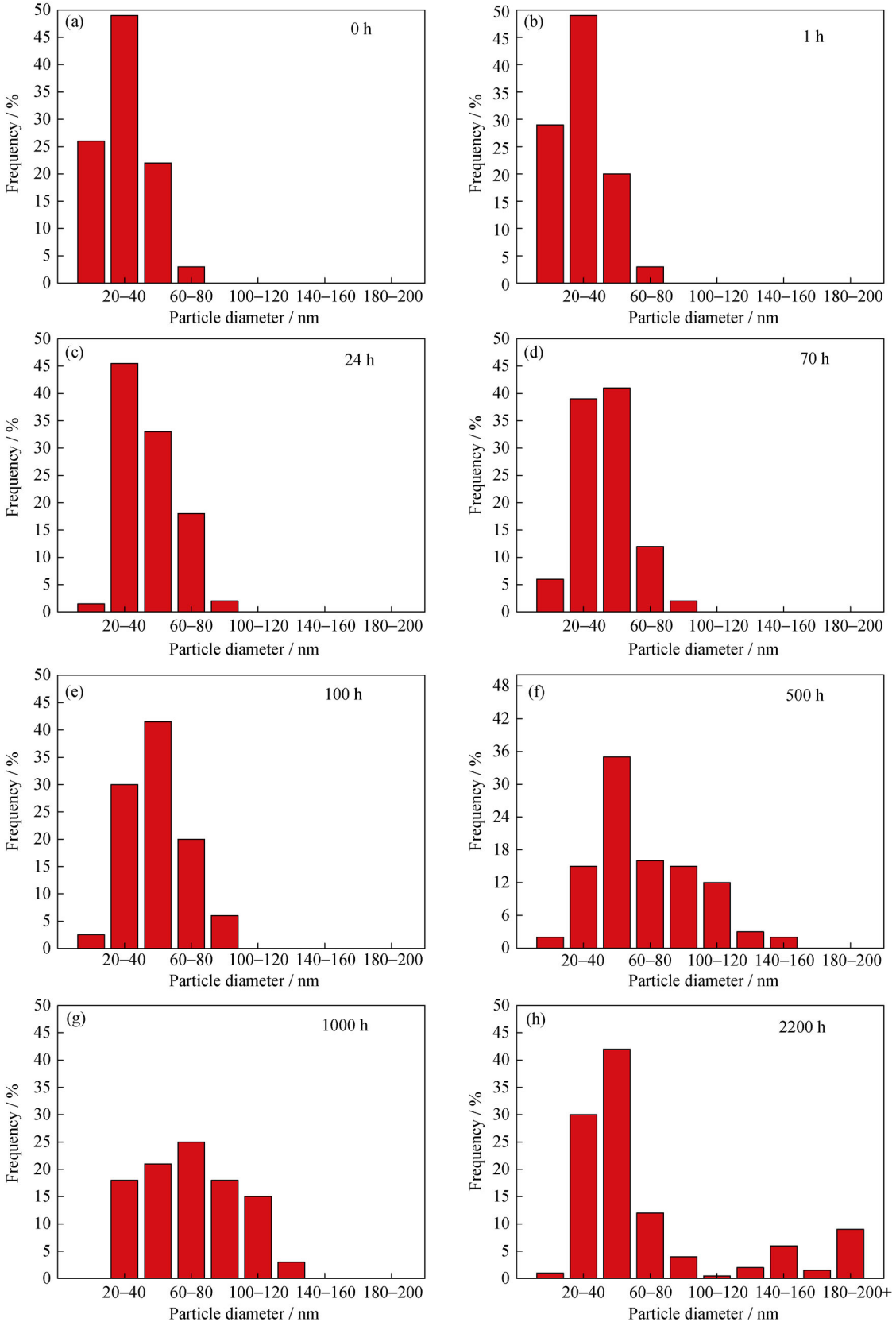

Fig. 5. Measured size distributions of MX carbonitrides in specimens aged at 700°C for different periods: (a) 0 h, (b) 1 h, (c) 24 h, (d) 70 h, (e) 100 h, (f) 500 h, (g) 1000 h, and (h) 2200 h.

Table 2. Measured size of MX carbonitrides in the investigated type 347H austenitic steel specimens aged at 700°C for different periods nm

Aging time / h	Maximum size	Minimum size	Mean size
0	76.5	11.3	18.7
1	86.5	12.1	23.7
24	90.9	13.6	33.5
70	105.8	10.4	42.9
100	106.7	13.5	46.1
350	112.0	16.9	54.4
500	140.3	17.9	58.7
1000	137.7	21.3	65.4
2200	254.3	11.9	85.8

Table 3. Measured mean size of investigated MX carbonitrides in type 347H austenitic steel subjected to different isothermal conditions nm

Aging time / h	Mean size			
	700°C	800°C	850°C	900°C
1	23.7	25.5	37.1	40.5
24	33.5	37.1	51.9	107.0
70	42.9	47.6	79.2	154.3
100	46.1	52.7	96.5	175.4

Although the size of Nb(C,N) carbonitrides is increased and the coarsening rate is expedited with increasing isothermal holding temperature, such conditions also facilitate the formation of secondary Nb(C,N) precipitates. These small particles maintain the properties of type 347H austenitic steel at high temperatures. According to the reference [15], diffusion distance is directly proportional to the square root of time; thus, the size variation of Nb(C,N) carbonitrides with aging time exhibits a parabola behavior (see Fig. 7(a)). Fig. 7(b) shows the frequency that the coarsening rate of Nb(C,N) is time-independent.

3.2. Coarsening rate and activation energy of MX carbonitrides

3.2.1. Coarsening rate

Studies have shown that precipitation strengthening can substantially improve the mechanical properties of steels. The equation describing the kinetics of isothermal treatment was derived by Lifshita, Slyozov, and Wagner and is known as the LSW equation. This equation has been widely used to calculate the particle coarsening kinetics [16–20]. The following assumptions were considered in the derivation of the LSW equation: (i) all particles are spherical, with a radius of r; (ii) all particles are much smaller than the average

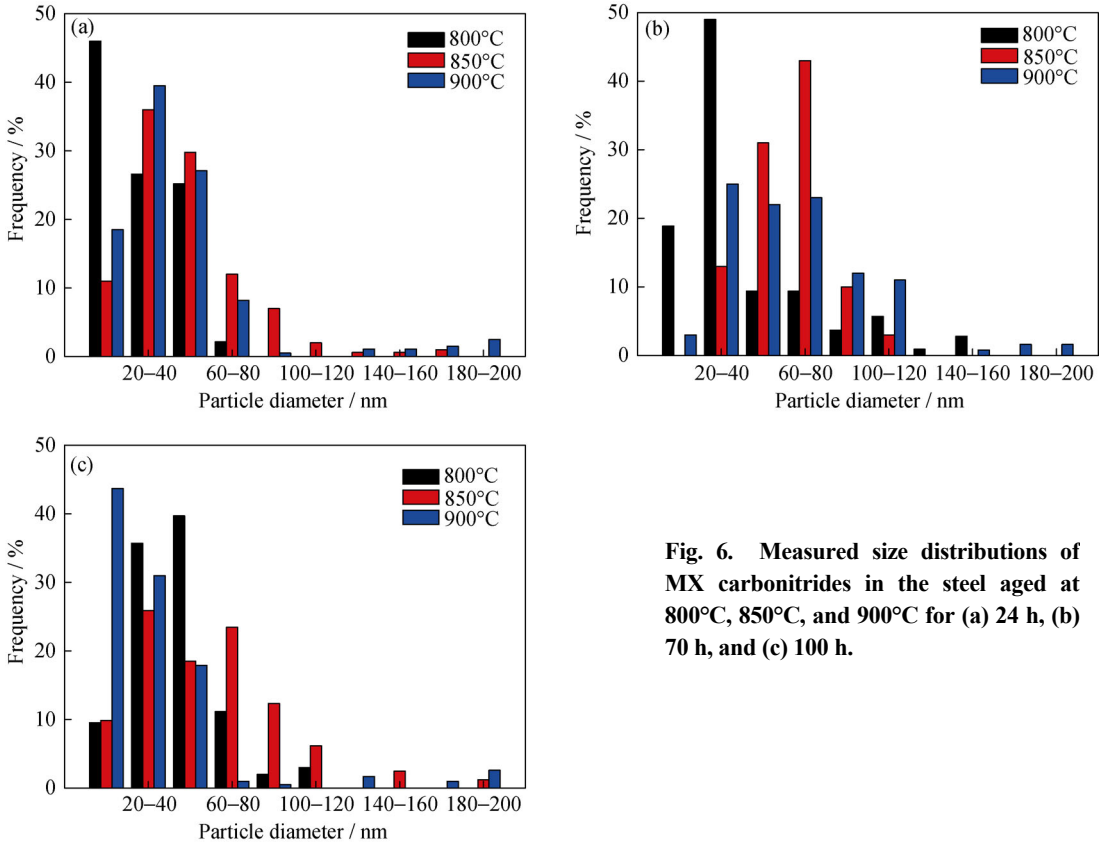

Fig. 6. Measured size distributions of MX carbonitrides in the steel aged at 800°C, 850°C, and 900°C for (a) 24 h, (b) 70 h, and (c) 100 h.

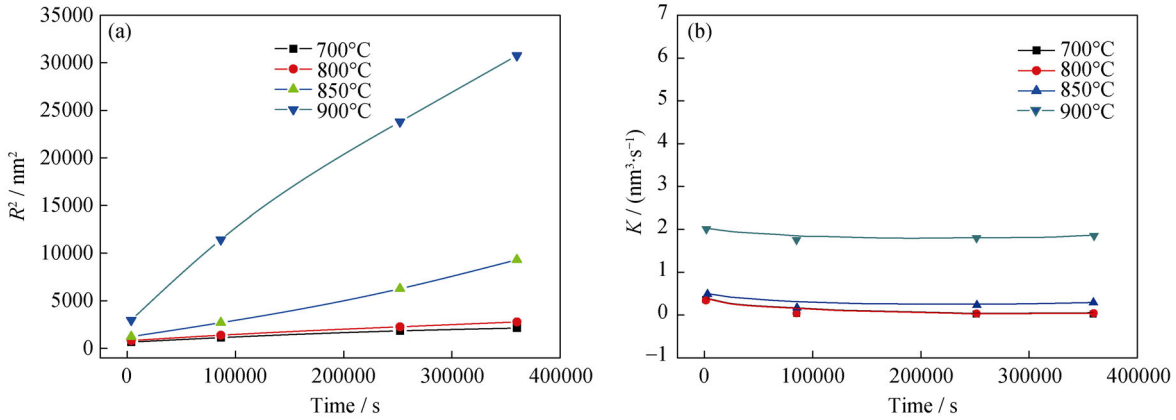

Fig. 7. (a) Measured average size of MX carbonitrides in the type 347H austenitic steel specimens aged at 700, 800, 850, and 900°C; (b) the calculated coarsening rate of MX carbonitrides during aging.

distance between particles; and (iii) particles do not interact. The third power of the particle radius r exhibits a linear relationship with time t. For a spherical particle, the coarsening kinetics governed by the diffusion of atoms is calculated according to Eq. (1):

$$r^3 - r_0^3 = \frac{8\Gamma C_e V_m^2 D}{9RT} = Kt \tag{1}$$

To extend this model to cubic particles, Refs. [20–21] revised and reformulated Eq. (1) as

$$a^3 - a_0^3 = \frac{8\Gamma C_e V_m^2 D}{9RT} = K't \tag{2}$$

where a is the half-length of the particle in nm, a_0 is the initial half-length of the particle in nm, r is the radius of the particle in nm, r_0 is original radius of the particle in nm, V_m is the molar volume, D is the diffusivity coefficient, Γ is the interfacial energy between the particle and the matrix, C_e is the equilibrium solute concentration, R is the gas constant, T the thermodynamic temperature, and K' is the coarsening rate in nm^3·s^{-1} with time t.

As indicated in Eq. (2), the coarsening rate of Nb(C,N) can be calculated when the size of the Nb(C,N) precipitates is known. Hence, the coarsening rates of Nb(C,N) carbonitrides in the type 347H austenitic steel samples under various aging conditions were obtained using Eq. (2) in conjunction with the measured size of Nb(C,N) precipitates listed in Table 2. The results reveal that the coarsening rate increases with increasing annealing temperature. Fig. 7(b) illustrates the thus-obtained coarsening rates as a function of the isothermal holding period. The coarsening rate of Nb(C,N) carbonitrides clearly increases with increasing annealing temperature and decreases with increasing annealing time. Because of the high isothermal annealing temperature, the fast diffusion rate of atoms leads to not only a decrease of the number of carbonitride particles but also a decrease of the mutual distance among the growing particles. At the same time, the solute concentration and matrix concentration decrease gradually, which greatly reduces the driving force for the diffusion of interfacial solute atoms [22–23]. Thus, the coarsening rate of Nb(C,N) carbonitrides is reduced accordingly.

3.2.2. Diffusion activation energy

In general, the diffusion coefficient is expressed as

$$D = D_0 \exp\left(-\frac{Q}{RT}\right) \tag{3}$$

where D is the diffusion coefficient in the austenite, D_0 is the original diffusion coefficient in the austenite, R is the gas constant, T is the thermodynamic temperature, and Q is the diffusion activation energy.

Substituting Eq. (3) into Eq. (2) and assigning $M = \frac{8\Gamma C_e V_m^2}{RT} D_0$ (C_e is assumed to be constant), we obtain a relation between $1/T$ and $R\ln(K't)$; furthermore, the diffusion activation energy Q can be determined by the slope of the linear region [24–27]:

$$R\ln(K't) = -Q\frac{1}{T} + R\ln M \tag{4}$$

Adopting the measured sizes of the precipitates presented in Table 4, we obtained the corresponding diffusion activation energies, as reported in Table 5. The best-fit straight lines of these points are shown in Fig. 8. The variation of the slope of the best-fit straight lines is large in the case of the specimens annealed in the temperature range from 800°C to 900°C. Furthermore, the slope of these best-fit straight lines for samples treated using different annealing periods exhibits a similar tendency. The slope of the best-fit straight lines is the diffusion activation energy of the Nb(C,N) carbonitrides. According to the references [28–31], the diffusion activation energies of C atoms, N atoms, and Nb atoms in γ-Fe are 85 kJ·mol^{-1}, 72 kJ·mol^{-1}, and 286·kJ mol^{-1}, respectively.

Table 4. Calculated coarsening rate of MX-type carbonitrides in type 347H austenitic steel subjected to different aging treatments ($nm^3 \cdot s^{-1}$)

Aging temperature / °C	Coarsening rate			
	1 h	24 h	70 h	100 h
700	0.37	0.05	0.04	0.03
800	0.36	0.07	0.05	0.05
850	0.52	0.19	0.24	0.31
900	2.03	1.76	1.82	1.87

Table 6 shows the calculated diffusion activation energies of the MX carbonitrides. When the isothermal temperature is 800–900°C, the mean diffusion activation energy of the Nb(C,N) carbonitrides is 294 $kJ \cdot mol^{-1}$. The calculated diffusion activation energy is similar to the diffusion activation energy of Nb atoms in γ-Fe, which suggests that the precipitation of Nb(C,N) carbonitrides is governed by the diffusion of Nb atoms at 800–900°C.

Table 5. Data used for the calculation of the diffusion activation energy of MX-type carbonitrides in type 347H austenitic steel

$(1/T)$ / 10^{-4} K^{-1}	$\ln(K' \times 3600)$	$\ln(K' \times 24 \times 3600)$	$\ln(K' \times 70 \times 3600)$	$\ln(K' \times 100 \times 3600)$
9.32 (800°C)	59.38	71.78	78.50	81.63
8.90 (850°C)	62.63	80.83	91.64	96.63
8.52 (900°C)	73.98	99.21	108.39	111.58

Note: The unit of K' is nm^3/s.

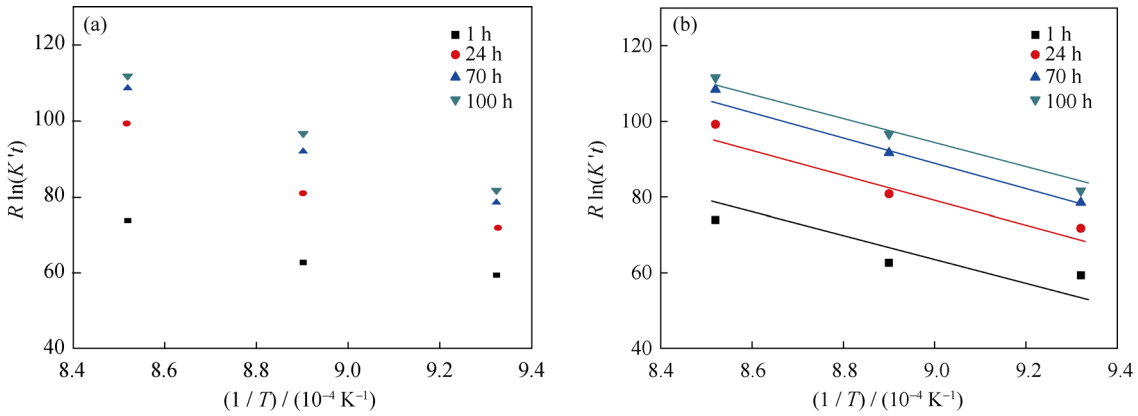

Fig. 8. (a) Measured scattergram and (b) regression curves for diffusion activation energy determination during the coarsening of MX carbonnitrides.

Table 6. Calculated diffusion activation energy (Q) during the coarsening of MX carbonitrides in type 347H austenitic steel

Temperature / °C	Time / h	Q / ($kJ \cdot mol^{-1}$)	Mean value of Q / ($kJ \cdot mol^{-1}$)
800–900	1	325	294
	24	262	
	70	250	
	100	337	

4. Conclusions

The coarsening behavior of MX carbonitrides in type 347H heat-resistant austenitic steel during thermal aging was investigated. The results are summarized as follows:

(1) MX carbonitrides, identified as Nb(C,N), were observed to be the primary precipitating phase in type 347H austenitic steel. The coarsening rate of Nb(C,N) carbonitrides was observed to increase with increasing isothermal holding temperature, whereas it was independent of the isothermal holding period.

(2) After measuring the size of the Nb(C,N) carbonitrides in the type 347H austenitic steel specimens, we calculated a diffusion activation energy for the growth of Nb(C,N) carbonitrides of 294 $kJ \cdot mol^{-1}$ at 800–900°C, which suggests that the growth mechanism of Nb(C,N) carbonitrides is controlled by the diffusion of Nb atoms in this temperature range.

Acknowledgements

The authors are grateful to the China National Funds for Distinguished Young Scientists (No. 51325401), the National High Technology Research and Development Program of China (No. 2015AA042504), and the National Natural Science Foundation of China (No. 51474156) for financial support.

References

[1] O. Prat, J. Garcia, D. Rojas, J.P. Sanhueza, and C. Camurri, Study of nucleation, growth and coarsening of precipitates in a novel 9% Cr heat resistant steel: experimental and modeling,

Mater. Chem. Phys., 143(2014), No. 2, p. 754.

[2] H. Chilukuru, K. Durst, S. Wadekar, M. Schwienheer, A. Scholz, C. Berger, K.H. Mayer, and W. Blum, Coarsening of precipitates and degradation of creep resistance in tempered martensite steels, *Mater. Sci. Eng. A*, 510-511(2009), p. 81.

[3] S.M. Hong, M.Y. Kim, D.J. Min, K.H. Lee, J.H. Shim, D.I. Kim, J.Y. Suh, W.S. Jung, and I.S. Choi, Unraveling the origin of strain-induced precipitation of $M_{23}C_6$ in the plastically deformed 347 austenite stainless steel, *Mater. Charact*., 94(2014), p. 7.

[4] H.B. Li, Z.H. Jiang, Z.R. Zhang, Y. Cao, and Y. Yang, Intergranular corrosion behavior of high nitrogen austenitic stainless steel, *Int. J. Miner. Metall. Mater.*, 16(2009), No. 6, p. 654.

[5] X.B. Hu, L. Li, X.C. Wu, and M. Zhang, Coarsening behavior of $M_{23}C_6$ carbides after ageing or thermal fatigue in AISI H13 steel with niobium, *Int. J. Fatigue*, 28(2006), No. 3, p. 175.

[6] F.R. Xiao, Y.B. Cao, G.Y. Qiao, X.B. Zhang, and B. Liao, Effect of Nb solute and NbC precipitates on dynamic or static recrystallization in Nb steels, *J. Iron Steel Res. Int*., 19(2012), No. 11, p. 52.

[7] L. Tan, T.S. Byun, Y. Katoh, and L.L. Snead, Stability of MX-type strengthening nanoprecipitates in ferritic steels under thermal aging, stress and ion irradiation, *Acta Mater*., 71(2014), p. 11.

[8] Y.T. Xu, M.J. Wang, Y. Wang, T. Gu, L. Chen, X. Zhou, Q. Ma, Y.M. Liu, and J. Huang, Study on the nucleation and growth of Laves phase in a 10% Cr martensite ferritic steel after long-term aging, *J. Alloys Compd*., 621(2015), p. 93.

[9] F. Shi, L.J. Wang, W.F. Cui, and C.M. Liu, Precipitation kinetics of Cr_2N in high nitrogen austenitic stainless steel, *J. Iron Steel Res. Int*., 15(2008), No. 6, p. 72.

[10] N.Q. Zhu, L. Lu, Y.L. He, L. Li, and X.G. Lu, Coarsening of $M_{23}C_6$ precipitates in an Fe–Cr–C ternary alloy, *J. Iron Steel Res. Int*., 19(2012), No. 9, p. 62.

[11] Å. Gustafson and M. Hättestrand, Coarsening of precipitates in an advanced creep resistant 9% chromium steel: quantitative microscopy and simulations, *Mater. Sci. Eng. A*, 333(2002), No. 1-2, p. 279.

[12] Å. Gustafson, Coarsening of TiC in austenitic stainless steel: experiments and simulations in comparison, *Mater. Sci. Eng. A*, 287(2000), No. 1, p. 52.

[13] K. Miao, Y.L. He, N.Q. Zhu, J.J. Wang, X.G. Lu, and L. Li, Coarsening of carbides during different heat treatment conditions, *J. Alloys Compd*., 622(2015), p. 513.

[14] J.W. Bullard, Numerical simulations of transient-stage Ostwald ripening and coalescence in two dimensions, *Mater. Sci. Eng. A*, 238(1997), No. 1, p. 128.

[15] S. Ghosh, Kinetic study on the coarsening behaviour of equilibrium phases in Nb alloyed ferritic stainless steels at 700°C, *Mater. Chem. Phys.*, 124(2010), No. 1, p. 13.

[16] O. Prat, J. Garcia, D. Rojas, C. Carrasco, and A.R. Kaysser-Pyzalla, Investigations on coarsening of MX and $M_{23}C_6$ precipitates in 12% Cr creep resistant steels assisted by computational thermodynamics, *Mater. Sci. Eng. A*, 527(2010), No. 21-22, p. 5976.

[17] J.N. Moon, H.C. Jeong, J.B. Lee, and C.H. Lee, Particle coarsening kinetics considering critical particle size in the presence of multiple particles in the heat-affected zone of a weld, *Mater. Sci. Eng. A*, 483-484(2008), No. 1-2, p. 633.

[18] S.G. Huang, R.L. Liu, L. Li, O. van der Biest, and J. Vleugels, NbC as grain growth inhibitor and carbide in WC–Co hardmetals, *Int. J. Refract. Met. Hard Mater.*, 26(2008), No. 5, p. 389.

[19] H.B. Li, Z.H. Jiang, H. Feng, Q.F. Ma, and D.P. Zhan, Aging precipitation behavior of 18Cr–16Mn–2Mo–1.1N high nitrogen austenitic stainless steel and its influences on mechanical properties, *J. Iron Steel Res. Int.*, 19(2012), No. 8, p. 43.

[20] M. Tsujikawa, N. Yamauchi, N. Ueda, T. Sone, and Y. Hirose, Behavior of carbon in low temperature plasma nitriding layer of austenitic stainless steel, *Surf. Coat. Technol*., 193(2005), No. 1-3, p. 309.

[21] H. Chilukuru, K. Durst, S. Wadekar, M. Schwienheer, A. Scholz, C. Berger, K.H. Mayer, and W. Blum, Coarsening of precipitates and degradation of creep resistance in tempered martensite steels, *Mater. Sci. Eng. A*, 510-511(2009), p. 81.

[22] Z.X. Xia, C. Zhang, and Z.G. Yang, Control of precipitation behavior in reduced activation steels by intermediate heat treatment, *Mater. Sci. Eng. A*, 528(2011), No. 22-23, p. 6764.

[23] K. Sawada, K. Kubo, and F. Abe, Creep behavior and stability of MX precipitates at high temperature in 9Cr–0.5Mo–1.8W–VNb steel, *Mater. Sci. Eng. A*, 319-321(2001), p. 784.

[24] M. Tamura, H. Sakasegawa, A. Kohyama, H. Esaka, and K. Shinozuka, Creep deformation of iron strengthened by MX type particles, *J. Nucl. Mater.*, 329(2004), No. 1, p. 328.

[25] M. Tamura, H. Sakasegawa, A. Kohyama, H. Esaka, and K. Shinozuka, Effect of MX type particles on creep strength of ferritic steel, *J. Nucl. Mater.*, 321(2003), No. 2-3, p. 288.

[26] T. Onizawa, T. Wakai, M. Ando, and K. Aoto, Effect of V and Nb on precipitation behavior and mechanical properties of high Cr steel, *Nucl. Eng. Des.*, 238(2008), No. 2, p. 408.

[27] O. Prat, J. Garcia, D. Rojas, C. Carrasco, and A.R. Kaysser-Pyzalla, Investigations on coarsening of MX and $M_{23}C_6$ precipitates in 12% Cr creep resistant steels assisted by computational thermodynamics, *Mater. Sci. Eng. A*, 527(2010), No. 21-22, p. 5976.

[28] J. Ågren, A revised expression for the diffusivity of carbon in binary FeC austenite, *Scripta Metall. Mater.*, 20(1986), No. 11, p. 1507.

[29] G.P. Krielaart and S. van der Zwaag, Kinetics of $\gamma \rightarrow \alpha$ phase transformation in Fe–Mn alloys containing low manganese, *Mater. Sci. Technol.*, 14(1998), No. 1, p. 10.

[30] W.F. Gale and T.C. Totemeir, *Smithells Metals Reference Book*, 8th Ed., Elsevier Butterworth-Heinemann, Waltham Massachusetts (United States), 2004, p. 13.

[31] M. Maalekian, R. Radis, M. Militzer, A. Moreau, and W.J. Poole, *In situ* measurement and modelling of austenite grain growth in a Ti/Nb microalloyed steel, *Acta Mater.*, 60(2012), No. 3, p. 1015.